Arab J Sci Eng (2014) 39:9127–9136
DOI 10.1007/s13369-014-1462-3

RESEARCH ARTICLE - MECHANICAL ENGINEERING

Natural Convection Between a Vertical Wall Exposed to Solar Energy and a Shaded Wall

A. A. Mohamad · H. Alansary · J. Orfi

Received: 28 May 2014 / Accepted: 30 September 2014 / Published online: 12 November 2014

Abstract The energy requirement for cooling residential and industrial buildings in the summertime is extensive, especially in hot weather countries. Solar energy contributes substantially to the cooling load. The solar intensity is usually high and can be about a kW/m^2. Besides, the cooling period or comfort conditions in those countries exceed 5 months and outdoor temperature can reach more than 40 °C. Any attempt to reduce the effect of solar energy on the cooling load is worthy of investigation. The present work analyzes using artificial, naturally ventilated, shading covers to reduce the effect of solar energy. A computational fluid dynamics approach is used to understand the physics of natural convection between an exterior wall of a building and an artificial shade. Since the building is air conditioned, it is expected that the exterior wall temperature may be less than the ambient temperature of a shaded wall. Hence, the analysis covered a wide range of rate of cooling of the exterior wall and assumed that the shading material is always at a higher temperature than the ambient due to solar energy.

Keywords Natural convection · Passive cooling · Building envelop · Shading · Solar energy

A. A. Mohamad (✉)
Department of Mechanical and Manufacturing Engineering, Schulich School of Engineering, The University of Calgary, Calgary, AB, Canada
e-mail: mohamad@ucalgary.ca

H. Alansary · J. Orfi
Department of Mechanical Engineering, King Saud University, Riyadh, KSA

الخلاصة

تستعمل الطاقة على نطاق واسع لتبريد المباني السكنية والصناعية في فصل الصيف ، وبخاصة في الدول التي تتميز بطقس حار. وتسهم الطاقة الشمسية إلى حد كبير في حمل التبريد. إن كثافة الطاقة الشمسية عادة ما تكون مرتفعة حيث تصل إلى حدود الكيلوات في المتر مربع. إضافة إلى أن الفترة التي يجب أن تكون فيها الأجواء مكيفة في هذه الدول الحارة تتجاوز الخمسة أشهر في السنة ودرجة حرارة الهواء الخارجي يمكن أن تصل إلى أكثر من 40 درجة مئوية (40°C) . وعليه فإن الحد من تأثير الطاقة الشمسية في حمل التبريد يستحق التحقيق. ويحلل هذا العمل الحد من تأثير الطاقة الشمسية في حمل التبريد ، وذلك باستعمال أغطية اصطناعية للتظليل.

ولفهم الظاهرة الفيزيائية للحمل الحراري بين جدار خارجي لبناية وظل اصطناعي وقع استعمال منهج حسابي لديناميكا الموائع. ونظرا لأن الهواء داخل البناية مكيفٌ فمن المتوقع أن تكون درجة حرارة الجدار الخارجي أقل من درجة حرارة الهواء المطلق لجدار مظلل. وبالتالي يغطي التحليل المعتمد في هذه الدراسة جزءا هاما لمعدل التبريد للجدار الخارجي ، وذلك بافتراض أن درجة حرارة المادة المستعملة للتظليل الاصطناعي تكون عادة أكبر من درجة حرارة الهواء المطلق وذلك بسبب تأثير الطاقة الشمسية.

List of symbols

H	Channel length
g	Gravitational acceleration
h	Wall heat transfer coefficient
k	Fluid thermal conductivity
L	Spacing between walls
N	Cooling rate $= (T_\mathrm{w} - T_\mathrm{a})/(T_s - T_\mathrm{a})$
Nu	Nusselt number
P	Dimensionless pressure
Pr	Prandtl number
Ra	Rayleigh number
T	Temperature
U	Dimensionless transverse velocity
V	Dimensionless streamwise velocity
X	Dimensionless transverse coordinate

Y Dimensionless axial coordinate
θ Dimensionless temperature, $(T - T_a)/(T_s - T_a)$
ν Kinetic viscosity

Subscripts

a Ambient air
av Average
s Hot wall
w Cold wall

1 Introduction

Buildings consume more than one-third of the world's energy [1], mainly for heating and cooling in cold and hot climate regions, respectively. In order to reduce energy consumptions, passive heating and cooling are more attractive [2, 3]. Extensive research has been done, especially in cold climates to reduce the demand for energy in the winter period by using under grounding energy source heating, solar energy, passive ventilations, etc. However, the problem of cooling is more challenging in hot and dry climate regions.

The energy needed for cooling and comfortable living in hot climate countries is vast, especially in the summertime. In those countries, solar energy drastically contributes to the cooling load, mainly through exposed roofs and south-facing walls. Any method that can reduce the effect of solar flux striking exterior walls of a building is worth considering.

Planting trees in front of walls exposed to solar energy, as natural shading, is effective and has been used [4]. Of course, planting trees is also esthetically appealing; however, it is not always feasible to plant trees in places where water is not accessible. Many techniques have been applied or explored to reduce the cooling load in the summertime. Those techniques include adding insulations, natural ventilations, painting the roof with reflective materials, long-wave radiative cooling, using green roofs (vegetation), using water ponds on the roof, evaporative cooling, etc. [5]. Some of the mentioned techniques have limited applications or drawbacks. For instance, water leaking may become a problem in case of a vegetated roof. Also, water is a valuable commodity and is of limited availability in certain regions, such as a desert region. Dust accumulation on the painted roof may limit the effectiveness of the paint reflectance and regular maintenance is needed. All the mentioned approaches are considered to be passive techniques.

Passive cooling techniques can be classified into three categories [6], namely solar and heat protection, heat modulation, and heat dissipation techniques. The current work fits the first category. Comprehensive review of the passive cooling techniques can be found in Givoni [6] and Santamouris [7].

The impact of shading on the cooling load and lighting was studied by Tzempelikos and Athienities [8] and Perez et al. [4]. Their studies indicated that proper shading can reduce the energy demand for cooling and lighting substantially, which depends on the climate conditions and orientation of the building. Performances of different passive cooling systems were considered by [9–17]. Ciampi et al. [18] used thermal resistance analysis to study the effect of air flow in ventilated facades. The analysis is sophisticated enough for designing ventilated facades for renovated and new buildings. They established criteria for energy-efficient facades. For complete thermofluid analysis, they indicated that there is a need for accurate knowledge of heat transfer coefficients, friction factors and thermophyiscal properties of the materials. On the other hand, Patania et al. [19,20] used a CFD turbulent model to study natural convection heat transfer and fluid flow between two vertical and inclined plates, respectively. Similar work was done by Fedorov and Viskanta [21]. The mentioned CFD analyses considered ascending flow, i.e., attention was not given to reverse flow, in other words; the temperatures of both heated walls were kept above the ambient temperature.

However, most of the works in open literature deal with natural convection between vertical plates maintained at temperatures higher than the ambient temperature. The detailed analysis of the physics of the natural convection between a shading sheet and a building is not fully explored [18,19], which is the topic of the current work. A computational approach was used to simulate natural flow and heat transfer in the gap between a vertical wall of a building and a vertical shading sheet. The flow is driven by the temperature gradient between the wall, shading plate and ambient (buoyancy force). Effects of the rate of heating and cooling of a building for specific values of Rayleigh's number are discussed. Streamlines, isotherms and rate of heat transfer as a function of the controlling parameters are illustrated and discussed. Furthermore, photovoltaic cells can be installed on the shading surface, which help in reducing cooling load and, at the same time, generate electricity for a different purpose. Furthermore, the natural convection from the back surface of the photovoltaic cells dissipates heat (cools the cells) and increases the efficiency of the cells.

2 Problem Definition and Governing Equations

Figure 1 shows the schematic diagram of the problem, which consists of two vertical, parallel plates. The bottom and top openings are exposed to ambient. The left hand plate is kept at a higher temperature (T_s) than the ambient temperature (T_a), while the right hand plate (T_w) is kept at a lower temperature than the ambient. Air is naturally driven by the buoyancy force between the plates. The aspect ratio (height to width)

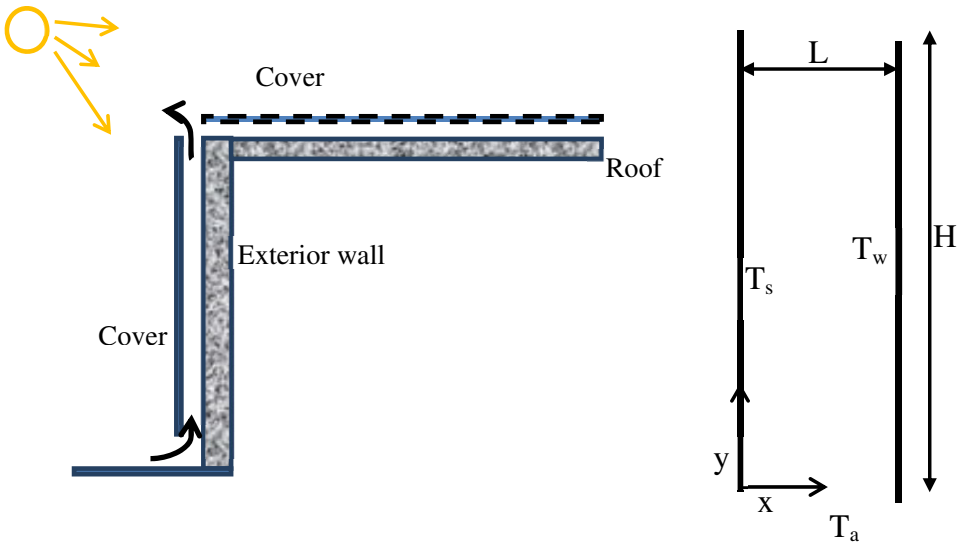

Fig. 1 Schematic diagram of the problem: **a** physical, **b** model

is set to ten, and air is assumed to have Prandtl number of 0.71. The aspect ratio of ten is selected based on the rationale that a 30 cm spacing between the wall and the shading plate is sufficient for a building of 3 m in height. The problem simulates natural convection through a gap between an air-conditioned room wall and a shading plate exposed to solar energy.

Governing equations are mass, momentum and energy equations. The flow is assumed to be two dimensional. The thermophysical properties of air are assumed to be constants, except density variation in buoyancy term, where Boussinesq approximation is assumed. Hence, the non-dimensional governing equation for laminar flow can be written as [22]:

Continuity

$$\frac{\partial U}{\partial X}+\frac{\partial V}{\partial Y}=0 \tag{1}$$

X-momentum

$$\frac{\partial}{\partial X}(UU)+\frac{\partial}{\partial Y}(VU)=-\frac{\partial P}{\partial X}+\frac{\partial^2 U}{\partial X^2}+\frac{\partial^2 U}{\partial Y^2} \tag{2}$$

Y-momentum

$$\frac{\partial}{\partial X}(UV)+\frac{\partial}{\partial Y}(VV)=-\frac{\partial P}{\partial Y}+\frac{\partial^2 V}{\partial X^2}+\frac{\partial^2 V}{\partial Y^2}+\frac{Ra}{Pr}\theta \tag{3}$$

Energy equation

$$\frac{\partial}{\partial X}(U\theta)+\frac{\partial}{\partial Y}(V\theta)=\frac{1}{Pr}\left(\frac{\partial^2\theta}{\partial X^2}+\frac{\partial^2\theta}{\partial Y^2}\right) \tag{4}$$

where, the gap width (L), kinematic viscosity divided by $L(\nu/L)$ and temperature difference between hot wall and ambient temperatures ($T_s - T_a$) are used in scaling, the length, velocity and temperature, respectively. For higher Rayleigh numbers, the standard $k-e$ turbulent model is used, the details of the modeling is given by [21].

It should be mentioned that since the temperatures of the walls are fixed, then the radiative heat transfer exchange between the surfaces of the walls can be calculated independently, assuming that the air is a non-participating medium. However, if the flux is given at the boundary, then a term of heat transfer by radiation should be added to the energy equation.

Boundary conditions

$$\text{At X} = 0 \quad \text{and} \quad \text{X} = 1.0, \quad \text{U} = \text{V} = 0. \tag{5a}$$

$$\text{At Y} = 0 \quad \text{and} \quad \text{Y} = 10, \quad \text{P} = 0.0 \tag{5b}$$

At $X = 0, \theta = 1.0$; at $X = 1.0, \theta = N$, where N set to $0, -0.2, -0.4, -0.6, -0.8$ and -1.0, depends on the cooling rate.

$$\text{At Y} = 0.0,\ \theta = 0 \quad \text{if V} > 0.0 \quad \text{or} \quad \frac{\partial\theta}{\partial Y}=0 \quad \text{if V} < 0.0. \tag{6a}$$

$$\text{At Y} = 10.0,\ \theta = 0 \quad \text{if V} < 0.0 \quad \text{or} \quad \frac{\partial\theta}{\partial Y}=0 \quad \text{if V} > 0.0. \tag{6b}$$

3 Similarity Transformation Analysis

Natural convection from a vertical plate exposed to a constant ambient temperature can be solved by similarity transformation of the above partial different equations (NS) into ordinary differential equations, which can be solved by Rang–Kutta method. For laminar flows ($Ra < 2 \times 10^8$), the thermal boundary can be obtained by similarity transformation and yields,

$$\delta = \frac{7y}{\left(\frac{Ra_H}{PR}\right)^{0.25}} \tag{7}$$

For $Ra = 10^8$ and for air ($Pr = 0.71$, $\nu = 1.5 \times 10^{-5}\,\mathrm{m^2/s}$, $\beta = 1/300\,\mathrm{K^{-1}}$, $\Delta T = 20\,^{\circ}\mathrm{C}$), y value can be calculated as,

$$Ra = \frac{g\,\beta \Delta T y^3}{\alpha \nu} = 10^8$$

y will be about 0.4 m and δ will be about 2.6 cm. Flow becomes turbulent for $Ra > 10^9$.

For turbulent air flow, the similarity analysis yields [23],

$$\delta = 0.57408 \left(\frac{\upsilon^2}{g\beta\Delta T}\right)^{0.1} y^{0.7} \tag{8a}$$

In non-dimensional form,

$$\frac{\delta}{H} = 0.57408 \left(\frac{Pr}{Ra_H}\right)^{0.1} \left(\frac{y}{H}\right)^{0.7} \tag{8b}$$

Assuming that the turbulent started from the leading edge and for wall of 4 m in height, the boundary layer thickness at the end of the plate is about 17 cm for above given conditions. However, as the Rayleigh number increases, the thermal boundary layer decreases. For instance, the boundary layer thickness is about 12 cm at four meters height and for $Ra = 10^{13}$. To confirm that Eq. (8) yields correct estimated, turbulent ($k - e$) mode CFD is used and boundary layer estimated.

For a gap of 25–30 cm between a building wall and shading, ensure that there will be no convective thermal communication between two boundaries for the laminar or for the turbulent flows. In other words, heat transfer between the building wall and shading plate is only by radiation. The radiation exchange between the two vertical surfaces mainly depends on the emissivity and absorptivity of the surfaces. The radiation flux exchange between two parallel gray surfaces can be expressed as,

$$q_{r=\frac{\sigma\left(T_s^4 - T_w^4\right)}{\frac{1}{\varepsilon_w} + \frac{1}{\varepsilon_s} - 1}} \tag{9}$$

where σ, ε_{w}, ε_s, T_{w}, and T_s are Stefan–Boltzmann constant, emissivity of the wall, emissivity of the shading material, wall temperature and shading surface temperature, respectively.

Most building materials have emissivity of 0.9 (except metal surfaces). If we assume that the shading plate temperature is about 60 °C (333 K) and wall temperature about 30 °C (303 K), the radiation exchange per unit $\mathrm{m^2}$ is about 179.5 W. For solar intensity of one kW, 179.5 is <18 %. In order to reduce the rate of radiation exchange, polished metals are highly recommended.

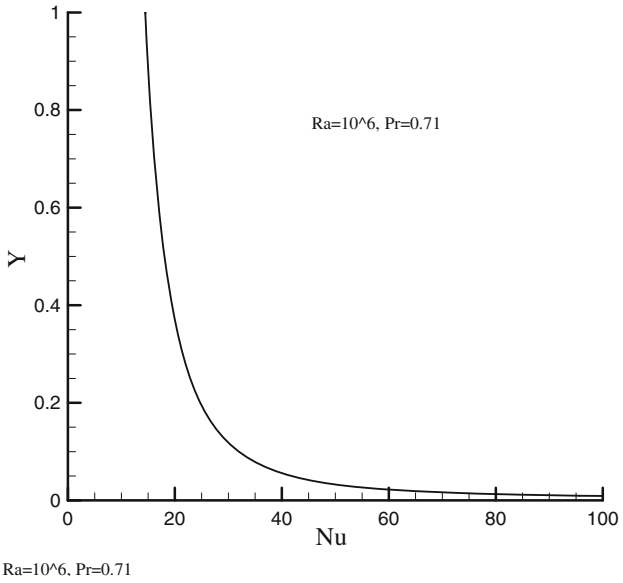

Ra=10^6, Pr=0.71

Fig. 2 Local Nusselt number variation along a heated wall, $Ra = 10^6$, $Pr = 0.71$

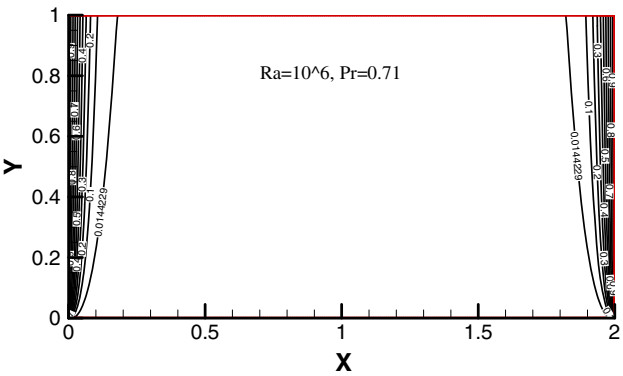

Fig. 3 Isotherms in a vertical channel with heated walls, $Ra = 10^6$, $Pr = 0.71$

4 Method of Solution and Code Validation

The Navier–Stokes equations (1–4) were solved by finite volume method for laminar and turbulent flows. For turbulent flow, low Reynolds number $k - e$ model is used.

In-house code was developed and tested for many problems [21,24,25]. Since, the method of solution was given in details in other publications, as mentioned, then there is no need to repeat it here. In order to insure reliable resolution of dependent variables, large number of control volumes are used, and the grids are clustered at the boundaries. The problem is not easy to deal with, because the velocity and temperature boundary conditions at the bottom and at the top of the system are not known prior to solution. However, imposing constant pressure at the inlet and exit boundaries yields correct results [24].

Natural convection along a vertical plat is simulated. The predicted Nusselt number for $Ra = 10^5, 10^6$ and 10^7 is

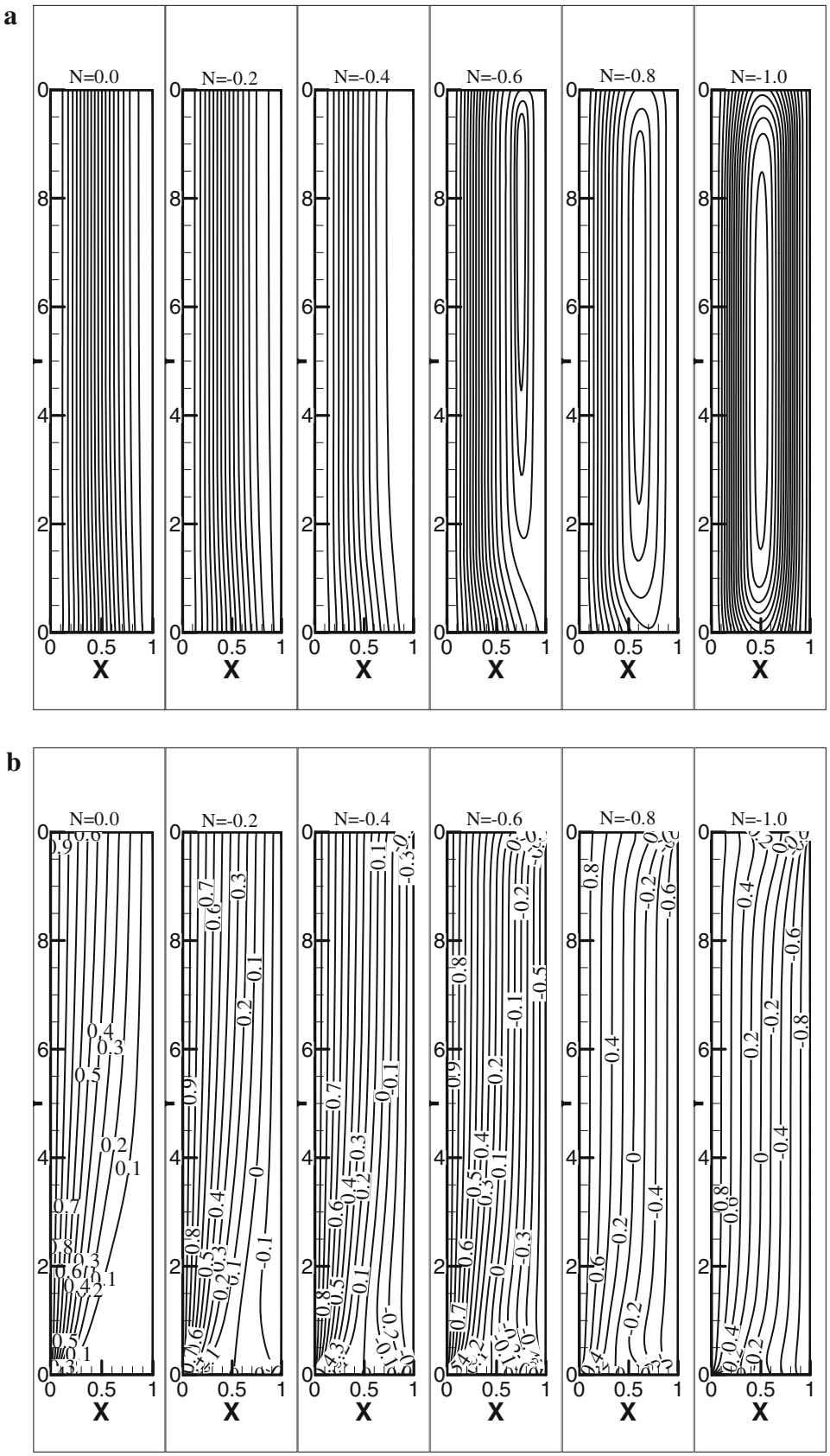

Fig. 4 **a** Streamlines in an open ended, differentially heated channel, $Ra = 10^3$, $Pr = 0.71$. **b** Isotherms in an open ended, differentially heated channel, $Ra = 10^3$, $Pr = 0.71$

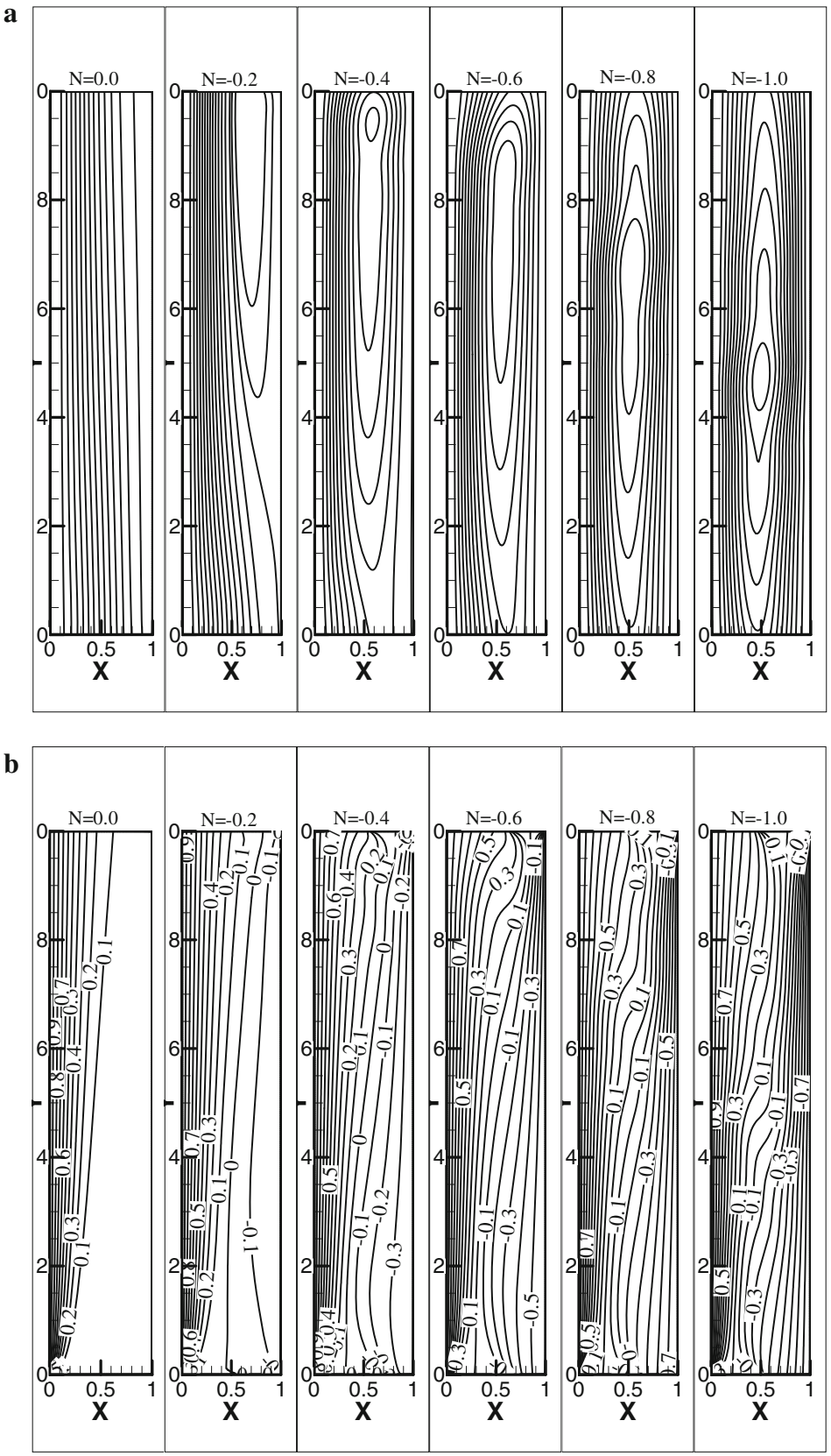

Fig. 5 **a** Streamlines in an open ended, differentially heated channel, $Ra = 10^4$, $Pr = 0.71$. **b** Isotherms in an open ended, differentially heated channel, $Ra = 10^4$, $Pr = 0.71$

14.25, 21.71 and 36.21, respectively. The published correlations (Churchill and Chu's correlation [26]) for $Ra = 10^5$, 10^6 and 10^7 are 9.82, 16.94 and 29.60, respectively. The code over predicted the Nusselt number by about 31, 22 and 18 %, for $Ra = 10^5$, $Ra = 10^6$ and 10^7, respectively, where extensively tested. The results presented were produced by using $1{,}601 \times 601$ non-uniform grids, where grids were clustered at boundaries of the domain. Also, different grid numbers were used to ensure that the results are grid size independent. For instance, the Nusselt numbers predicted for $Ra = 10^6$ are 21.026 and 21.71 for grid numbers of 201×201 and 401×401, respectively. The following states the reason that causes the difference between numerical predication and published correlation. The heat transfer (Nusselt number) is very high at the leading edge of the plate, then exponentially decreases along the plate, as the thermal boundary develops. The length of the leading edge is in the order of a few millimeters, which is difficult to measure Nusselt number at this region experimentally due to lateral heat conduction and size of the region, Fig. 2. This may explain the difference between predicted results and suggested correlations. In order to further explain the difference, if we ignore the leading edge difference, then the numerical predictions match the correlation results.

Figure 3 shows the ascending flow between the plates, which is expected. The dimensionless thermal boundary layer at the upper edge of the plate is 0.2, which is in very well agreement with the similarity solutions for laminar flow, Eq. (5).

The second test was carried out by keeping the plates at the same temperature but cooler than the ambient temperature. The predicted results were the same as before except the flow reversed its direction from ascending to descending flow. This test ensured that the open boundaries conditions are correctly set up.

5 Natural Convection Between a Wall and Shading Plate

The finite volume method is used to simulate natural convection through the gap between two vertical boundaries. The main objective of using CFD is to understand the flow pattern and temperature field between the shading and the building walls. The code was tested for a few natural convection problems. Hence, there is no need to repeat the details of the methodology of solution (interested readers can find the details in [21,24,25]). If the air flows toward the domain, the outdoor temperature is imposed at the boundary; if the flow is leaving the domain, the temperature at the boundary is set to the temperature of the internal, adjustment node to the boundary [24], i.e., the temperature gradient is set to zero. The results are presented for $Ra = 10^3$, 10^4 and 5×10^4, assuming flow is laminar. The results for $Ra = 10^5$ were

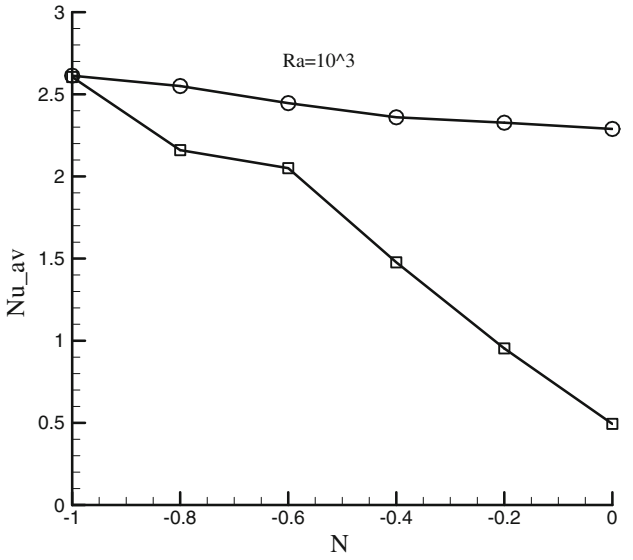

Fig. 6 Variation of average Nusselt with N for $Ra = 10^3$, $Pr = 0.71$, (*circle* for heated wall and *square* for cold wall)

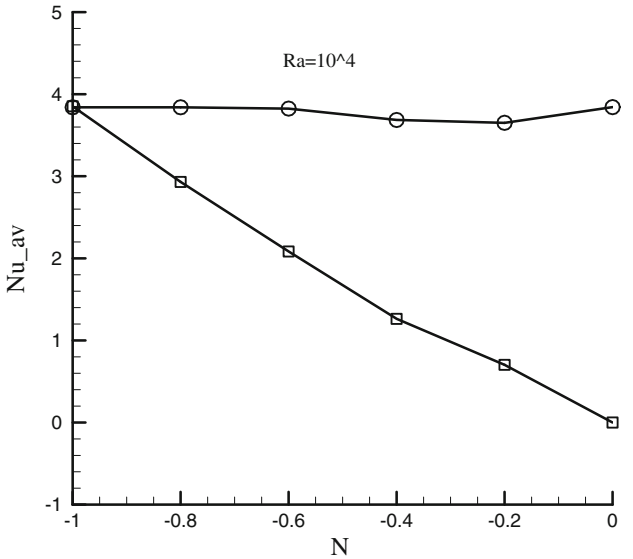

Fig. 7 Variation of average Nusselt with N for $Ra = 10^4$, $Pr = 0.71$, (*circle* for heated wall and *square* for cold wall)

fluctuating and unstable. It should be mentioned that Ra was based on the gap between the plates. To scale the problem based on the height of the plates instead of the gap, the mentioned Rayleigh number should be multiplied by 1,000. For instance, $Ra = 10^5$ based on the gap spacing is equal to 10^8 based on the height of the plates. It is expected that natural convection become unstable for Ra about 10^8. This may explain the instability of the results at $Ra = 10^5$. Therefore, for higher Ra numbers, turbulent model was used.

Figure 4a, b shows streamlines and isotherms for $Ra = 10^3$. For $N = 0$, where the building boundary (exterior wall) is passive and the case simulates a natural convection between

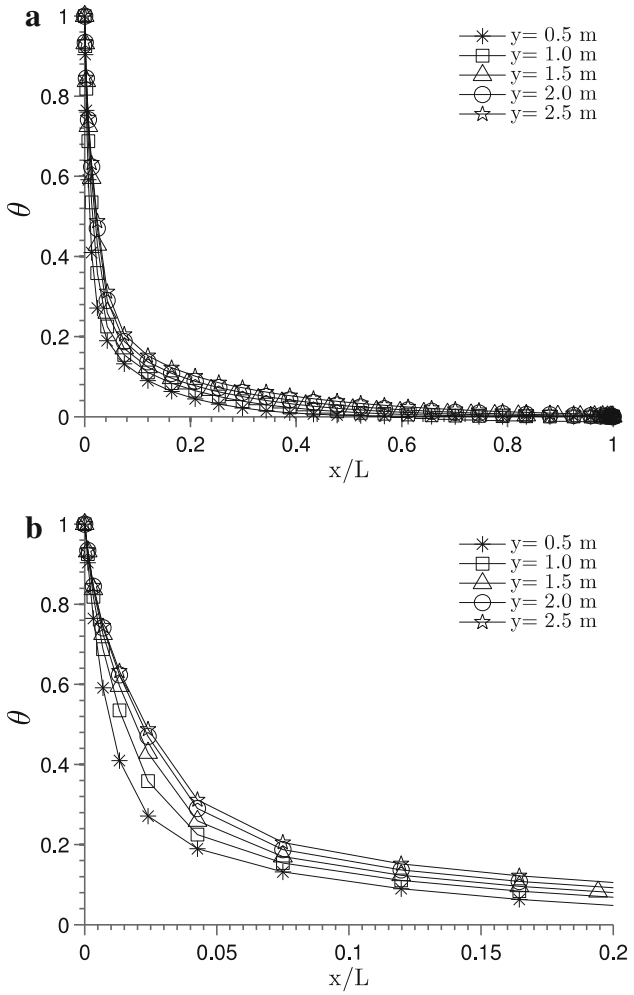

Fig. 8 **a** Dimensionless temperature distribution at different cross sections along the gap between the heated and cold plats, $Ra = 10^{10}$ and $Pr = 0.71$. **b** Same as Fig. 8a magnified near the heated boundary, $Ra = 10^{10}$ and $Pr = 0.71$

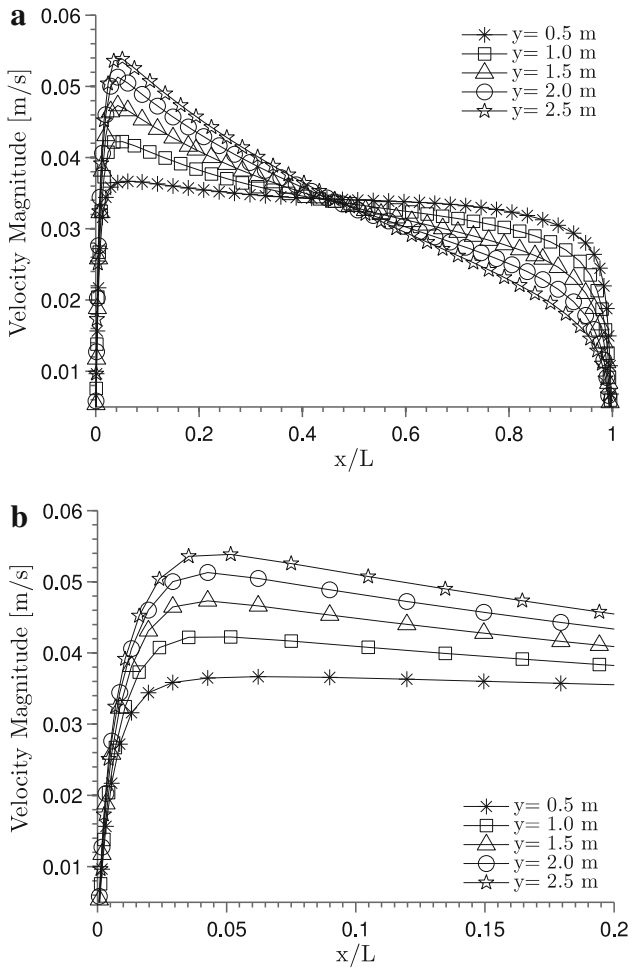

Fig. 9 **a** Vertical velocity profiles at different cross sections along the gap, for $Ra = 1 \times 10^{10}$, $Pr = 0.71$. **b** Same as Fig. 9a magnified near the heated boundary, $Ra = 1 \times 10^{10}$, $Pr = 0.71$.

a heated wall and a wall at ambient temperature. The flow is ascending through the gap (Fig. 4a). The effect of the cold wall is not that significant until $N = -0.4$, where reverse flow (descending) along the cold wall is clear. The strength of descending flow increases and N increases in the negative sense. At $N = -1.0$, where the rate of heating of the left hand wall is equal to rate of cooling on the right hand wall, the rate of ascending and descending flows is equal and most flow recirculates between the walls (Fig. 4a). Isotherms displayed in Fig. 4b shows a typical boundary layer development for $N = 0$. As N increases in negative sense, cold flow penetrates toward the hot wall.

Increasing Ra number to 10^4, based on the gap between plates (equal to 10^7, based on the height of the channel), the reverse flow becomes clearly evident at $N = -0.2$ (Fig. 5), while for $Ra = 10^3$, the reverse flow showed at $N = -0.6$ (Fig. 4). Also, a recirculated flow appears at the top end of the channel at $N = -0.4$. The reason that reverse flow intensified at $N = -0.2$ can be explained on the fact that Ra number based on the cold wall temperature is increased to 2.0×10^4, for $Ra = 10^4$ (based on the hot wall temperature). While for $Ra = 10^3$ (based on hot wall temperature), the reverse flow was evident at $N = -0.6$, i.e., $Ra = 6.0 \times 10^3$ (based on the cold wall temperature). Hence, it is expected that the effect of the cold wall penetrated deeper as the Ra number increases. Results obtained up to $Ra = 5 \times 10^4$. While results obtained for $Ra = 10^5$ were not stable, most probably, the flow became transient or turbulent.

Figures 6 and 7 show averaged Nusselt numbers for $Ra = 10^3$ and $Ra = 10^4$, respectively. It is clear that the rate of heat transfer, Nusselt number, from the hot wall is not that affected by the rate of cooling of the cold wall. However, the Nusselt number shows a slight increase as the rate of cooling of the wall increased. This can be explained with the fact that effect Rayleigh number increased because the temperature of air surrounding the heated plate decreased. The rate of heat transfer from the cooling plate almost linearly

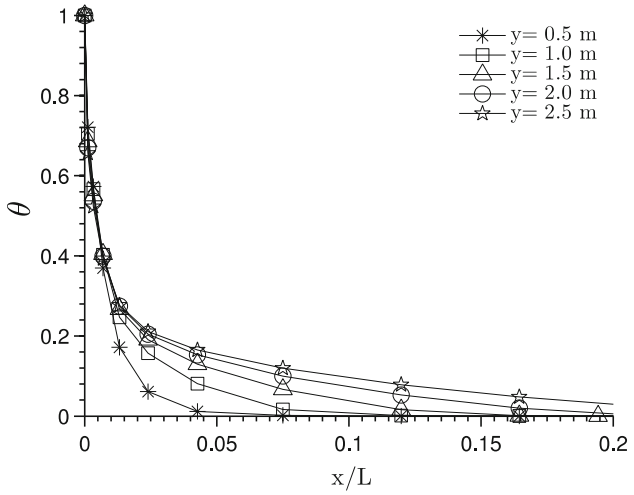

Fig. 10 Dimensionless temperature distribution at different cross sections along the gap between the heated and cold plats, $Ra = 10^{13}$ and $Pr = 0.71$

increased as the cooling rate increased. This is due to the fact that the Rayleigh number based on the cold plate and ambient temperature increases as the cooling rate increases. As the Rayleigh number increases, the thickness of the thermal boundary layer decreases. It is found that the heat transfer from both walls is decoupled at $Ra = 10^4$. In other words, despite the height, at some location between the walls, the temperature is equal to the ambient temperature (Fig. 5b).

For a higher Rayleigh number, the turbulent model is used. The results are presented for $Ra = 10^{10}$ and 10^{13} for natural convection between two plates. One plate is assumed to be heated by solar energy, and other plate is maintained at the ambient temperature. Figures 8, 9 and 10 show the predictions of turbulent mode. The results show that thermal boundary layer thickness at height of 2.5 m are 0.5 and 0.2 (scaled by the gap width, L) for $Ra = 10^{10}$ and 10^{13}, respectively. Hence, the results are consistent with analytical solution.

6 Conclusions

It is found that as the cooling rate and/or Rayleigh number increases the strength of the reverse flow increases. The rate of cooling insignificantly affected the rate of heat transfer from the heated wall. Increasing the cooling rate increases the rate of heat transfer from the cold wall. It is found that the heat transfer coefficient (Nusselt number) between the heated wall (outside wall) and air in the gap is not a strong function of the cooling rate of the cold wall. However, Nusselt number somehow linearly increases as the cooling rate of the cold wall (inner) increases. Also, the work clearly shows that natural convection between the walls is a complex phenomenon due to reverse flow. For a high Rayleigh number (greater than 10^4), the heat transfer from walls is decoupled. Hence, heat transfer from each wall can be calculated by considering heat transfer from a vertical plate exposed to ambient conditions.

References

1. Hong, T.; Yang, L.; Hill, D.; Feng, W.: Data and analytics inform energy retrofit of high performance building. Appl. Energy **126**, 90–106 (2014)
2. Artmann, N.; Manz, H.; Heislberg, P.: Climatic potential for passive cooling of buildings by night-time ventilation in Europe. Appl. Energy **84**, 187–201 (2007)
3. Eicker, U.: Cooling strategies, summer comfort and energy performance of a rehabilitated passive standard office building. Appl. Energy **87**, 2031–2039 (2010)
4. Perez, G.; Rincon, L.; Vila, A.; Gonzalez, J.M.; Cabeta, L.F.: Green vertical systems for buildings as passive systems for energy savings. Appl. Energy **88**, 4854–4859 (2011)
5. Santamouris, M.; Assimakopoulos, D. (eds.): Passive Cooling of Buildings. James and James Science Publishers, London (1996)
6. Givoni, B.: Passive and Low Energy Cooling of Building. Wiley, USA (1994)
7. Santamouris, M.: Passive Cooling of Buildings, Advances of Solar Energy, ISES. James and James Science Publishers, London (2005)
8. Tzempelikos, A.; Athienitis, A.K.: The impact of shading design and control on building and lighting demand. Sol. Energy **81**(3), 369–382 (2007)
9. Nahar, N.M; Sharma, P.; Purohit, M.M: Performance of different passive techniques for cooling of buildings in arid regions. Build. Environ. **38**, 109–116 (2003)
10. Alvarado, L.L; Martinez, E.: Passive cooling of cement-based roofs in tropical climates. Energy Build. **40**, 358–364 (2008)
11. Oliveira, J.T; Hagishima, A.; Tanimoto, J.: Estimation of passive cooling efficiency for environmental design in Brazil. Energy Build. **41**, 809–813 (2009)
12. Muselli, M.: Passive cooling for air-conditioning energy savings with new radiative low-cost coatings. Energy Build. **42**, 945–954 (2010)
13. Kumar, S.J; Tiwari, G.N; Bhagat, N.C.: Amalgamation of traditional and modern cooling techniques in a passive solar house: a design analysis. Energy Conversat. Manag. **35**(8), 671–682 (1994)
14. Theodosiou, T.G.: Summer period analysis of the performance of a planted roof as a passive cooling technique. Energy Build. **35**(9), 909–917 (2003)
15. Jürges, W.: The heat transfer at a flat wall (Der Wärmeübergang an einer ebenen Wand). Beiheftezum Gesundh.-Ing. **1**(19–23) (1924)
16. Defraeya, T.; Blocken, B.; Carmeliet, J.: Convective heat transfer coefficients for exterior building surfaces. Energy Convers. Manag. **52**(1), 512–522 (2011)
17. DeBlois, J.; Bilec, M.; Shaefer, L.: Simulating home cooling load reductions for a novel opaques roof solar chimney configuration. Appl. Energy **112**, 142–151 (2013)
18. Ciampi, M.; Leccese, F.; Tuoni, G.: Ventilated facades energy performance in summer cooling of buildings. Sol. Energy **75**, 491–502 (2003)
19. Patania, F.; Gagliano, A.; Nocera, F.; Ferlito, F.; Galesi, A.: Thermofluid-dynamic analysis of ventilated facades. Energy Build. **42**, 1148–1155 (2010)
20. Patania, F.; Gagliano, A.; Nocera, F.; Ferlito, A.; Galesi, A.: Energy analysis of ventilated roof. In: Howlett, R.J.; Jain, L.C.; Lee, S.H. (eds.) Sustainability in Energy and Buildings, SIST 7, pp. 15–23. Springer, Berlin (2011)

21. Fedorov, A.G.; Viskanta, R.: Turbulent natural convection heat transfer in an asymmetrically heated, vertical parallel-plate channel. Int. J. Heat Mass Transf. **40**(16), 3849–3860 (1997)
22. Pletcher, P.; Tannehill, J.C.; Anderson, D.A.: Computational Fluid Mechanics and Heat Transfer. CRC Press, Tayler and Francis Group, New York (2013)
23. Bergman, T.L.; Lavine, A.S.; Incropera, F.P.; DeWitt, D.P.: Fundamentals of Heat and Mass Transfer. Wiley, New York (2011)
24. Mohamad, A.A.: Natural convection from open cavities and slots. Numer. Heat Transf. A **27**, 705–716 (1995)
25. Sezai, I.; Mohamad, A.A.: Suppressing free convection from a flat plate with poor conductor ribs. Int. J. Heat Mass Transf. **42**, 2041–2051 (1998)
26. Churchill, S.W; Chu, H.H.S.: Correlation equations for laminar and turbulent few convection from a vertical plate. Int. J. Heat Mass Transf. **18**, 1323–1329 (1975)